Virology 442 (2013) 3–11

Contents lists available at SciVerse ScienceDirect

Virology

journal homepage: www.elsevier.com/locate/yviro

Mapping the telomere integrated genome of human herpesvirus 6A and 6B

Jesse H. Arbuckle [a,b], Shara N. Pantry [a], Maria M. Medveczky [a], Joshua Prichett [c], Kristin S. Loomis [c], Dharam Ablashi [c], Peter G. Medveczky [a,*]

[a] Department of Molecular Medicine, University of South Florida College of Medicine, Tampa, FL 33612, United States
[b] Molecular Genetics Section, Laboratory of Viral Diseases, National Institutes of Health, Bethesda, MD, United States
[c] The HHV-6 Foundation, Santa Barbara, CA, United States

ARTICLE INFO

Article history:
Received 4 January 2013
Returned to author for revisions
14 March 2013
Accepted 30 March 2013
Available online 4 May 2013

Keywords:
HHV-6
Human herpesvirus 6
CIHHV-6: chromosomally integrated human herpesvirus 6
PBMC
Peripheral blood mononuclear cells
Integration
Telomere
Telomere integration
single telomere length analysis
STELA

ABSTRACT

Human herpesvirus 6B (HHV-6B) is the causative agent of roseola infantum. HHV-6A and 6B can reactivate in immunosuppressed individuals and are linked with severe inflammatory response, organ rejection and central nervous system diseases. About 0.85% of the US and UK population carries an integrated HHV-6 genome in all nucleated cells through germline transmission. We have previously reported that the HHV-6A genome integrated in telomeres of patients suffering from neurological dysfunction and also in telomeres of tissue culture cells. We now report that HHV-6B also integrates in telomeres during latency. Detailed mapping of the integrated viral genomes demonstrates that a single HHV-6 genome integrates and telomere repeats join the left end of the integrated viral genome. When HEK-293 cells carrying integrated HHV-6A were exposed to the histone deacetylase inhibitor Trichostatin A, circularization and/or formation of concatamers were detected and this assay could be used to distinguish between lytic replication and latency.

Introduction

Herpesviruses are ubiquitous and have adapted a balance of lytic and latent infection within the infected host. Human herpesvirus 6 (HHV-6) was isolated from B-lymphocytes of patients with lymphoproliferative disorders while coinfected with HIV and HTLV (Salahuddin et al., 1986). Further molecular studies as well as sequencing of clinical isolates determined that humans carry two different viral species: HHV-6A and HHV-6B (Ahlqvist et al., 2005; Dominguez et al., 1999; Gompels et al., 1995; Yamanishi et al., 1988).

Human herpesvirus 6B (HHV-6B) primary infection in young children is the etiological agent of exanthema subitum (roseola infantum), which is characterized by high fever, diarrhea, and a mild skin rash along the trunk, neck, and face (Asano et al., 1994; Yamanishi et al., 1988). Serologic studies have found that by the age of two, greater than 90% of children have acquired a primary HHV-6A/B infection (Okuno et al., 1989; Zerr et al., 2005). HHV-6A has been associated with several adult diseases and various neurological disorders including encephalitis, ataxia, seizures, multiple sclerosis, Hashimoto's thyroiditis, and has been implicated as a cofactor in AIDS progression (Ablashi et al., 2010; Ahlqvist et al., 2005; Cameron et al., 2010; Caselli et al., 2012; De Bolle et al., 2005; Donati et al., 2003; Jones et al., 1994; Lusso et al., 2007, 1989; Yamashita and Morishima, 2005; Yao et al., 2010). Nevertheless, the causal link between human disease and HHV-6A infection remains to be fully elucidated.

The viral genome of HHV-6B is 162 kbp long, encompassing 119 unique open reading frames (ORF), while HHV-6A genome contains 119 unique ORF and is 159 kbp long (Dominguez et al., 1999; Gompels et al., 1995). The genome of HHV-6A and HHV-6B is organized into two major regions (Fig. 1a). The unique (U) region of the genome is 143 kbp and comprises seven major core gene blocks that are conserved amongst Herpesviridae. The second major genomic regions of HHV-6A and HHV-6B are the ~8 kbp of left and right direct repeats (DR) located at the termini of the U region (Dominguez et al., 1999; Gompels et al., 1995). Within the right end direct repeat (DR_R) and the left end direct repeat (DR_L)

Abbreviations: HHV-6, human herpesvirus 6; CIHHV-6, chromosome integrated human herpesvirus 6; PBMCs, peripheral blood mononuclear cells; STELA, single telomere length analysis.

* Correspondence to: University of South Florida College of Medicine, 12901 Bruce B. Blvd., MDC Box 7, Tampa, Fl. 33612. Fax: +1 813 974 7357.
E-mail address: pmedvecz@health.usf.edu (P.G. Medveczky).

0042-6822/$ - see front matter © 2013 Elsevier Inc. All rights reserved.
http://dx.doi.org/10.1016/j.virol.2013.03.030

the HHV-6A/HHV-6B genome encodes perfect and imperfect TTAGGG telomere repeat arrays.

Primary infection of HHV-6A/B leads to an increase in viral copies present in peripheral blood and subsequent decrease in viral copies during latency (Asano et al., 1994; De Bolle et al., 2005; Okuno et al., 1989; Yamanishi et al., 1988; Zerr et al., 2005). Following primary infection, the genome of most herpesviruses establishes latency as multi-copy circular episomes within the nucleus of the infected cell (reviewed by Pellett and Roizman, 2007). The expression of latent viral genes allows the stable replication and persistence of the latent viral episomes. However, no multi-copy episomes were detected in latently infected HHV-6A and 6B cells (Arbuckle et al., 2010). Through the use of fluorescent *in situ* hybridization (FISH), Gardella gel, Southern hybridization, and direct sequencing of viral integration sites from patient tissues and establishment of *in vitro* integrated cell lines our laboratory has demonstrated that HHV-6A specifically integrates into telomeres of chromosomes (Arbuckle et al., 2010; Arbuckle and Medveczky, 2011). These experiments suggest that homologous recombination occurs between the perfect TTAGGG telomere repeat arrays encoded in DR_R of HHV-6A genome with the subtelomere of the human chromosome.

In approximately 0.8% of the US and UK general population, high copies of HHV-6 genomes can be detected in peripheral blood measuring greater than 0.5 million copies per ml of blood and referred to as chromosomally integrated HHV-6 or CIHHV-6 (Arbuckle et al., 2010; Hall et al., 2008, Leong et al., 2007; Ward et al., 2006; Ward et al., 2005). Furthermore, Luppi et al. (1993) identified a unique high molecular weight viral fragment present in PBMCs of three patients with elevated copies of HHV-6. This high molecular weight fragment resolved by pulse field gel electrophoresis demonstrated one of the earliest observations of HHV-6 integration into the human genome. Subsequently, several other labs have suggested integration of HHV-6 into human chromosomes through FISH and HHV-6 DNA sequences were detected in hair follicles, lymph node, spleen, kidney, brain, liver, and cardiac tissues by PCR (Daibata et al., 1998; Jarrett et al., 1988; Nacheva et al., 2008; Strenger et al., 2010; Ward et al., 2006; Arbuckle et al., 2010).

In this study we set out to further map the genome structure of chromosome integrated HHV-6A and 6B. Here we show that similarly to HHV-6A, the HHV-6B genome integrates into telomeres of human chromosomes near the subtelomere via the perfect TTAGGG telomere repeat array encoded in DR_R of the viral genome. Single telomere length analyses (STELA) suggest that the physical end of chromosome harboring the integrated virus comprises telomeric repeats of variable length similar to those found in normal chromosomes. Finally, latently infected HEK-293 cells containing integrated viral genome were exposed to the histone deacetylase inhibitor Trichostatin A. Circularization and/or formation of concatamers were detected by a novel PCR assay indicating reactivation of HHV-6 from latency.

Results

HHV-6B integrates in telomeres in vitro

Since we have previously demonstrated the genome of HHV-6A integrates into telomeres of human chromosomes (Arbuckle et al., 2010), we hypothesized that the genome of HHV-6B would as well integrate into the telomeres of chromosomes during the course of infection. Furthermore, the T-cell line Molt3 is routinely used to propagate HHV-6B, yet we observed that cell lysis was often incomplete and many cells survived after the peak of productive infection possibly due to latent infection. DNA was isolated from HHV-6B infected Molt3 cells and PCR amplified for the putative viral genome-chromosome telomere junctions using subtelomere based primers (2p, 11q, 12q, 17p, and 18q) and a primer annealing to the right end of HHV-6B DR_R (Fig. 1b).

The primer to DR_R was utilized since our previously published results determined that HHV-6A *in vivo* and *in vitro* integration occurs through the linkage of perfect telomere array encoded in DR_R with the telomere sequence directly adjacent to the end of the chromosome (Fig. 1b) (Arbuckle et al., 2010). Amplified fragments from the subtelomeres of 2p, 11q, 12q, 17p, and 18q were fractionated on an agarose gel and Southern hybridization was performed with [γ^{32}P]-ATP-radiolabeled TTAGGG probe that hybridizes to both chromosome and HHV-6B telomere sequences located at their termini. As illustrated in Fig. 1c, PCR amplification coupled with Southern hybridization identified the linkage of the DR_R of HHV-6B genome with the telomere of specific chromosomes during *in vitro* infection of Molt3 cells.

To confirm the specific integration of HHV-6B into the telomere of chromosomes 2p, 11q, and 18q, we first cloned the PCR amplified fragments through pCR®4-TOPO® cloning system. Following transformation of competent cells, positive clones were identified by colony hybridization with [γ^{32}P]-ATP-radiolabeled HHV-6B and telomere oligonucleotide probes. Sequencing of clones confirmed *in vitro* infection of Molt3 cells resulted in the HHV-6B genome covalently linked with the telomere of chromosomes 2p, 11q, and 18q (Figs. 1d and S1). Therefore, the results from these experiments illustrate that similar to HHV-6A (Arbuckle et al., 2010), HHV-6B also specifically integrates into telomeres of chromosomes during the course of infection through the perfect telomere repeat array encoded in the DR_R of the viral genome.

Mapping the DR_L from the integrated HHV-6 genome

Results in the previous section and publications by our group identified the integration of HHV-6B and HHV-6A occurs through recombination with the perfect telomere repeats encoded in the DR_R (Fig. 1) (Arbuckle et al., 2010; Arbuckle and Medveczky, 2011). Therefore, we sought to further characterize the genomic structure of the integrated HHV-6A and HHV-6B genomes through mapping of the DR_L region and determine whether the tandem array of telomere repeats [$(TTAGGG)_n$] was extended beyond the DR_L (Figs. 1b and 2a). During the process of integration into chromosome telomeres, it is unknown whether recombination occurs with the DR_L perfect or imperfect telomere repeats (Fig. 1a and b). If recombination occurs through the perfect telomere repeats, the DR_L could potentially be lost during the process of telomere integration. To map various portions of the integrated viral genome in patients with CIHHV-6, we developed two PCR based assays to determine whether the entire DR_L is present or absent (Fig. 2a).

In the first experiment, amplification of the DR_L was completed by using primers that annealed to the DR_L and unique region of the integrated genome (Fig. 2a, Primer 1=P1 and Primer 2=P2), which effectively amplified across the perfect telomere repeat (Fig. 2a, short dark square). Genomic DNA isolated from Family-1 members with CIHHV-6 (Arbuckle et al., 2010) was subjected to this PCR based assay. The DR_L was successfully amplified as shown by Southern hybridization with telomere specific oligonucleotide probe (Fig. 2b).

To confirm the results in the previous experiment, we evaluated the DR_L in a second group of patients with inherited HHV-6 and utilized a second primer set (P3 and P4) in combination with *DraI* restriction enzyme digestion (Fig. 2a). The PCR amplified DR_L fragment has two *DraI* restriction sites that lead to the expected fragment sizes of 1027, 217, 186 bp according to the CIHHV-6A genome (strain U1102) (Gompels et al., 1995). Similarly to the

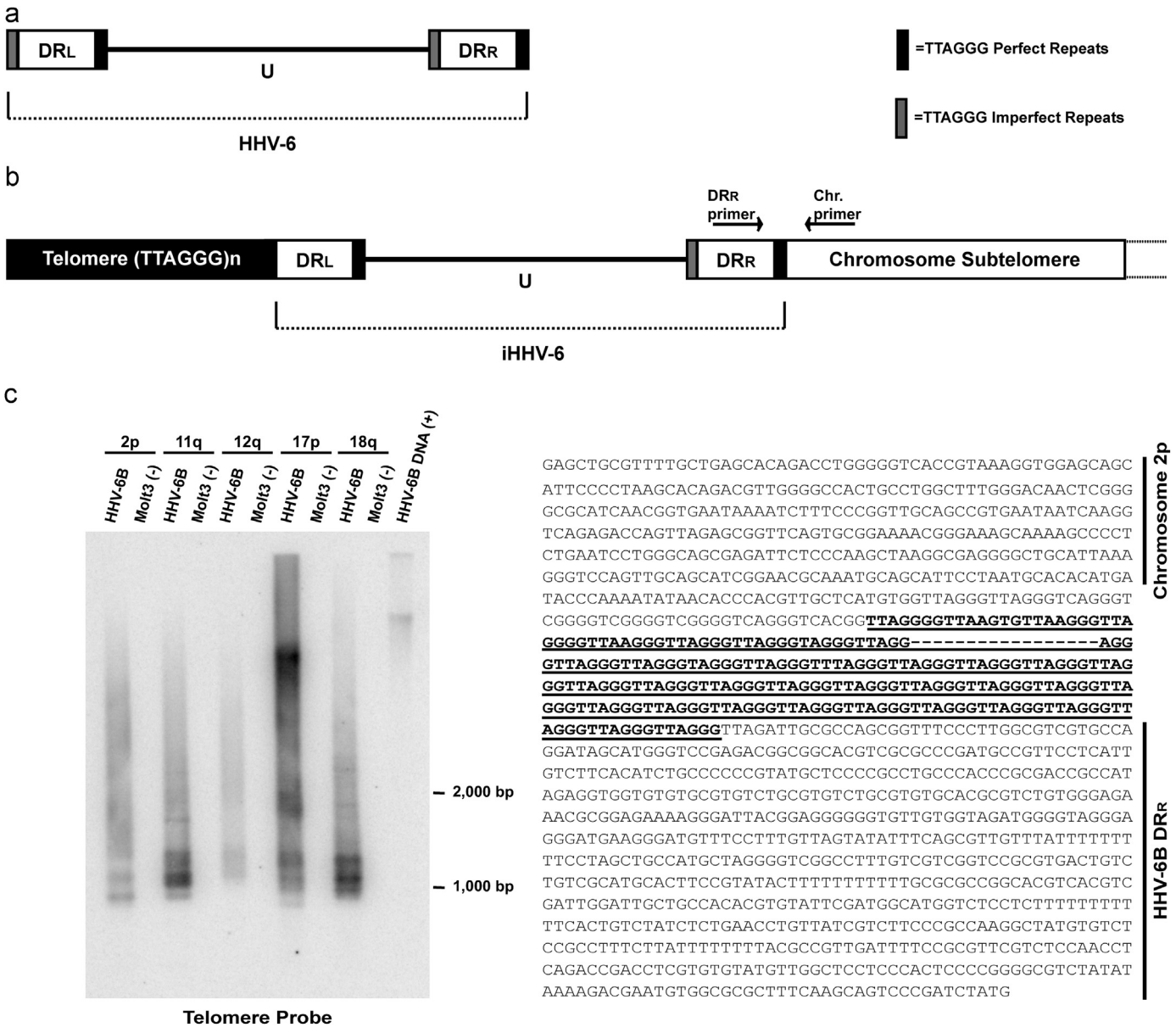

Fig. 1. Amplification of subtelomere-HHV-6B junction fragments from *in vitro*-infected Molt3 cells. (a) Genome structure of HHV-6B and HHV-6A in which unique (U) region is surrounded by left and right direct repeats (DR_L and DR_R) containing perfect (dark bars) and imperfect (shaded bars) telomere repeats. (b) The putative model of the integrated HHV-6-chromosome structure. Arrows indicate position of primers derived from the DR_R of the HHV-6 genome and from a specific chromosome subtelomere. (c) DNA from HHV-6B (strain Z29) infected and uninfected Molt3 cells were subjected to amplification by PCR primers derived from HHV-6B DR_R and subtelomere primers 2p, 11q, 12q, 17p and 18q (primer positions depicted in Fig. 1b). PCR products from virus-chromosome telomere junction were separated by electrophoresis and analyzed by Southern blot hybridization utilizing a ^{32}P-labeled telomere oligonucleotide probe. (d) DNA sequencing results of cloned fragments ($n=3$) of chromosome 2p subtelomere (upper) joined with TTAGGG telomere repeats (bold and underlined), and HHV-6B DR_R sequence (lower) during viral integration into chromosome telomere. Additional sequencing results are shown in Fig. S1.

results in Fig. 2b, the 1027 bp DR_L fragment was present in the inherited CIHHV-6 genome of all patients as this fragment hybridized with the oligonucleotide probe corresponding to the *DraI–DraI* fragment (Fig. 2c). In summary, results demonstrate the conservation of the CIHHV-6 DR_L segment.

Telomere repeats are covalently linked to the DR_L of integrated HHV-6 genome

The next series of experiments were designed to determine whether a tandem array of telomere repeats [$(TTAGGG)_n$] at the end of the chromosome is linked to the DR_L of the integrated HHV-6 genome. We adapted the methodology of Baird et al. single telomere length analysis (STELA) assay (Baird et al., 2003; Britt-Compton et al., 2006) to amplify and estimate the overall telomere length from a specific chromosome end (Fig. 3a). Genomic DNA was isolated from PBMCs of patients with inherited CIHHV. Next, a oligonucleotide linker (Tellorette-2) containing a single TTAGGG repeat was ligated to the end of the telomere by incubating 60 ng and 150 ng of genomic DNA with T4 ligase for 13 h at 35 °C (Fig. 3a). Linker-ligated DNA was amplified with a high fidelity Taq polymerase, linker annealing primer (P1), and a HHV-6 primer annealing to the DR_L (P2). The specific amplification of the chromosome telomere was identified through Southern

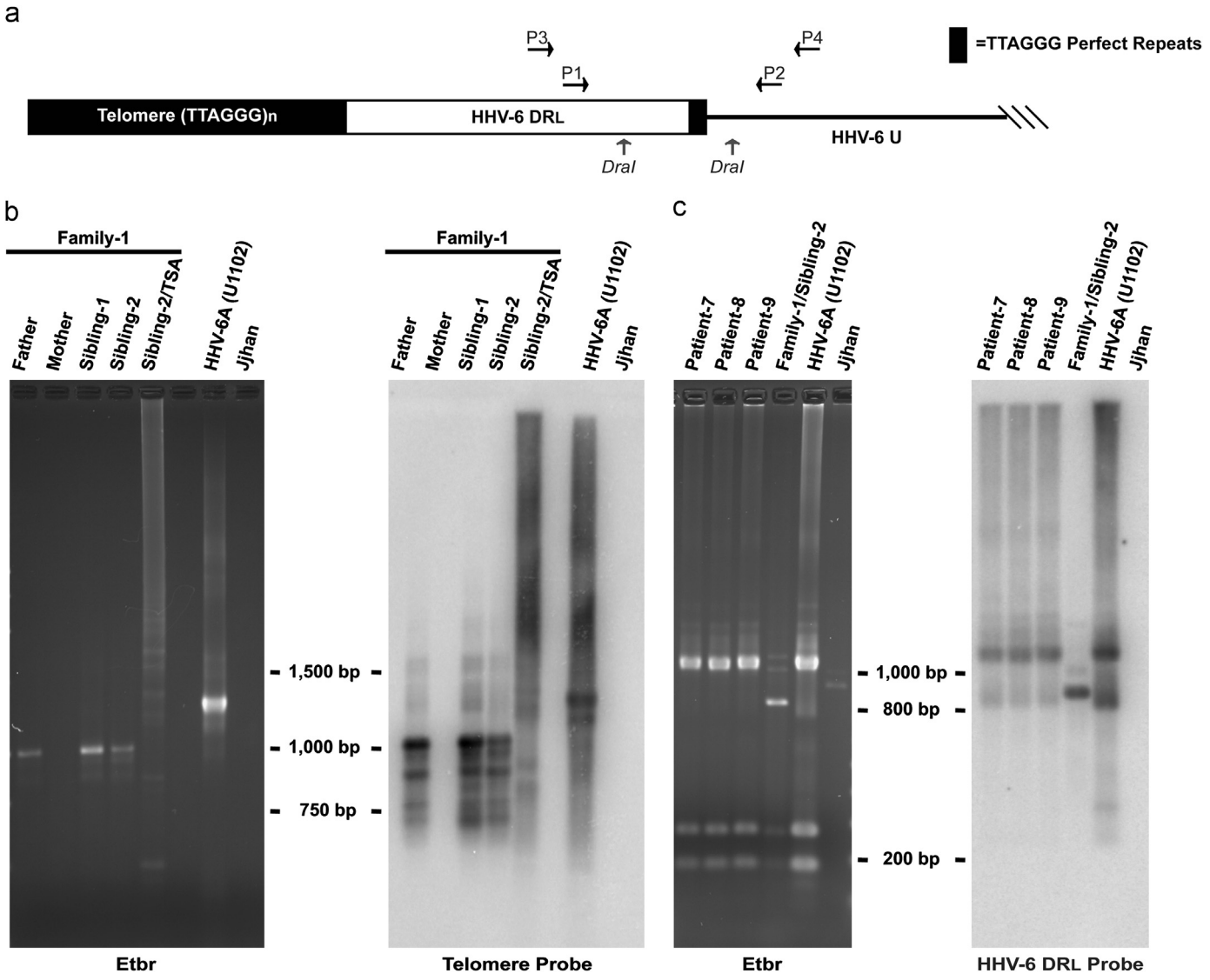

Fig. 2. Amplification and restriction enzyme digestion of DR_L fragments from DNA isolated from PBMC of members of a family with CIHHV-6. DNA from PBMC of members of Family-1 (Arbuckle et al., 2010) carrying HHV-6A integrated in telomere of chromosome 18q, Patients 7–9 carrying HHV-6B integrated, and Jjhan cell line infected with HHV-6A U1102 was subjected to PCR amplification using primer pairs as depicted. (a) Diagram for the amplification of DR_L in which primer 1 (P1) and 3 (P3) bind to regions inside DR_L and primer 2 (P2) and 4 (P4) binds within the U of HHV-6. *DraI* restriction sites are indicated by arrows. (b) Amplification of DR_L with primers P1 and P2 from members of Family-1 results in the predicted size of 1,198 bp (HHV-6A U1102) as shown in the ethidium bromide (Etbr) staining (left panel). Southern hybridization with telomere oligonucleotide probe (right panel). Controls: HHV-6A (U1102) positive control while Family-1/Mother and Jjhan were negative controls. (c) Amplification and restriction digestion with *DraI* results in the predicted 1027, 217, 186 bp (HHV-6A U1102) as shown in the ethidium bromide (Etbr) staining (left panel). Southern hybridization with HHV-6 DR_L oligonucleotide probe hybridizes with DR_L 1027 bp band (right panel). Controls: HHV-6A (U1102) infected Jjhan DNA positive control and Jjhan negative control.

hybridization with [γ^{32}P]-ATP-radiolabeled telomere oligonucleotide probe (Fig. 3b–d). Subsequently, the nitrocellulose blot was then stripped and re-hybridized with PCR amplified fragment from the viral DR_L. Co-hybridization of bands with telomere and DR_L probes confirmed the covalent linkage of chromosome telomere with the DR_L of inherited HHV-6 genome (Fig. 3a). Moreover, similar results were also obtained in STELA analysis of HEK-293 cell line harboring integrated HHV-6A (Fig. 3d). Heterogeneous banding pattern was observed when DNA from uninfected HEK-293 and Jjhan cells were subjected to STELA of chromosome Xp (Fig. S2). The heterogeneity of PCR amplified telomere fragments with the STELA assay has also been previously observed by Baird et al. in control human cells (Baird et al., 2003; Britt-Compton et al., 2006); this heterogeneity is likely due to the amplification of telomeres from a mixed populations of cells that contain variable lengths of telomeric sequence. The wide range of telomere length heterogeneity has been described by several other methods (reviewed by Lauzon et al., 2000).

Next using the STELA assay we determined the specific telomere length of DNA isolated from PBMCs of patients with inherited CIHHV-6A integrated into chromosome 17p. Calculation of the mean molecular weight of all bands co-hybridizing with telomere and DR_L (HHV-6A) radiolabeled probes from eight different PCR reactions was according to the protocol of Baird et al. (2003) and Britt-Compton et al. (2006). The mean telomere length of Sibling-2 and Sibling-1 was 5158 bp and 6309 bp, respectively (Fig. 3b and c). Therefore, the structure of the *in vivo* and *in vitro* integrated HHV-6A/B genome is as follows: chromosome-subtelomere-$(TTAGGG)_n$-DR_R-U-DR_L-$(TTAGGG)_n$ (Fig. 3a).

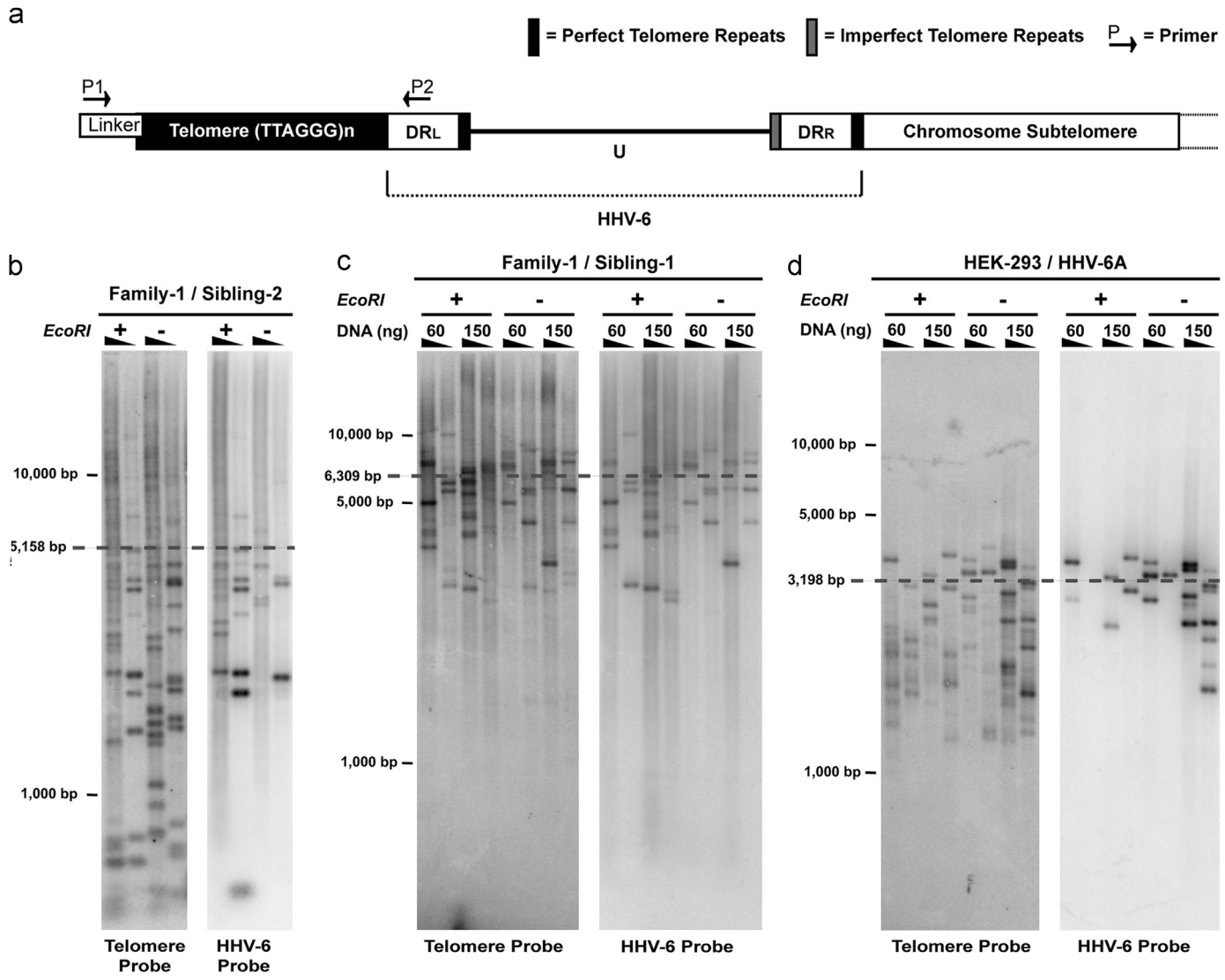

Fig. 3. STELA of DR_L adjoining telomere in PBMCs of *in vivo* integrated HHV-6 and *in vitro* integrated HEK-293 cells. (a) Diagram illustrating the strategy of single telomere length analysis (STELA) (Baird et al., 2003; Britt-Compton et al., 2006). To amplify the specific chromosome telomere extended beyond the DR_L of the integrated HHV-6 genome a linker (Telorette-2) oligonucleotide is ligated to the end of the telomere. The Telorette-2 ligation reaction contained 60 or 150 ng genomic DNA (*EcoRI* digested +/− for DNA solubilization). From this initial ligation, both ligation reactions are then serially diluted two-fold (indicated by the triangles in panels b, c and d) and subsequently amplified with primers P1 and P2. Genomic DNA isolated from PBMCs from CIHHV-6A individuals mapped to chromosome 17p13.3 was subjected to STELA; (b) sibling-2, and (c) sibling-1 of Family-1 (Arbuckle et al., 2010). (d) STELA was also performed on HEK-293 cells harboring telomere-integrated HHV-6A strain U1102 (Arbuckle et al., 2010). In each figure, mean telomere length is calculated from co-hybridization of telomere (left panel) and HHV-6 probes (right panel).

Trichostatin A promotes formation of circular/catenated viral genomes in latently infected cells

In our previous study we have demonstrated the histone deacetylase inhibitor Trichostatin A (TSA) can induce reactivation of the integrated CIHHV-6A viral genome from individuals' PBMCs as well as latently infected cell lines as evidenced by increase in viral DNA copies upon exposure to the TSA (Arbuckle et al., 2010). We hypothesized that reactivation of integrated CIHHV-6 genome resulted in formation of circular replication intermediates and/or tandem catenated forms of the genome as described for HHV-6 (Dominguez et al., 1999) and with other herpesviruses (Jacob et al., 1979; Poffenberger and Roizman, 1985). To test this hypothesis, HEK-293 cells latently infected and harboring integrated HHV-6A (strain U1102) (Arbuckle et al., 2010) were cultured in the presence of TSA at concentrations ranging from 10 ng/ml to 160 ng/ml for 3 days. Detection of viral episomes and/or concatemers was performed by PCR amplification of the DR by two primers that annealed to either end of the unique region of HHV-6A genome (Fig. 4a). Thus, amplification of DR would only occur during circularization or catenation of the viral genome in a head-to-tail conformation (Borenstein and Frenkel, 2009; Borenstein et al., 2010; Jacob et al., 1979; Martin et al., 1991; Poffenberger and Roizman, 1985; Severini et al., 2003). PCR products were subjected to sequential Southern hybridization with oligonucleotide probes to telomere, DR, and U regions of HHV-6A. The autoradiograms revealed that all three probes hybridized with PCR products of variable length from DNA isolated from cells that were treated with TSA (Fig. 4b, hybridization with telomere probe is shown) and not from control unstimulated or uninfected cells. Furthermore, similar variable fragments were also detected in control HHV-6A infected Jjhan cells. The amplification of variable size bands is likely due to insertion of variable number of telomere repeats in the DR during reactivation mediated by homologous recombination with telomere sequences. The absence of catenated genomes in latently infected cells also indicates that only a single genome integrates in telomeres. We studied two additional HEK-293 cell lines latently infected with HHV-6 and harboring telomere

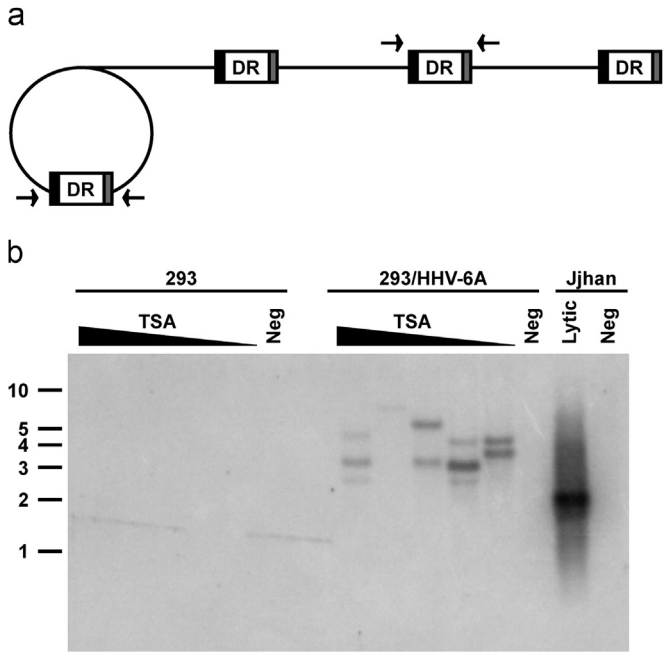

Fig. 4. Treatment of HHV-6A latently integrated HEK-293 cells with the histone deacetylase inhibitor TSA induces novel PCR products consistent with episome and/or concatemer formation during induction of lytic viral DNA replication. (a) Schematic illustration of rolling-circle replication of HHV-6 results in the formation of concatemers of viral genomes. Arrows indicate the location of primers utilized in the amplification of DR. (b) Latently infected, single-cell cloned and uninfected control HEK-293 cells were cultured with TSA at concentrations of 160 ng/ml, 80 ng/ml, 40 ng/ml, 20 ng/ml and 10 ng/ml and without drug treatment (Neg) for 3 days. DR amplification and Southern hybridization with DR oligonucleotide probe demonstrate the induction of DNA fragments amplifiable with the primers in DNA from cells treated with TSA. No amplification was detected in untreated 293/HHV-6A or 293 cells (Negative controls). Bands of variable size were also detected in DNA from Jjhan cells cultures infected with HHV-6A.

integrated U1102 virus described by Arbuckle et al. (2010), but no evidence for circularization/catenation was detected after TSA induction presumably due to integration of defective viral genomes (data not shown).

Discussion

The integration of HHV6-B and HHV-6A into the telomeres of human peripheral mononuclear cells *in vivo* and following *in vitro* infection of Jjhan T-cells, Molt3 T-cells, and HEK-293 cells is demonstrated (Fig. 1) (Arbuckle et al., 2010; Arbuckle and Medveczky, 2011). It appears that in cell lines capable of supporting productive, lytic infection, some of the cells quickly become latently infected through chromosomal integration, and remain viable. Thus, HHV-6B and HHV-6A integration is not an unusual dead-end phenomenon as described for other herpesviruses, but an alternative mechanism of achieving latency.

These results suggest that HHV-6B and HHV-6A integrate into the host genome via homologous recombination with human telomeres. In particular, integration of HHV-6B and HHV-6A occurs through recombination of the perfect telomere repeats encoded in the DR_R juxtaposed to the subtelomeric end of the chromosome (Figs. 1, S1, and 2) (Arbuckle et al., 2010). Moreover, the tandem array of telomere repeats [$(TTAGGG)_n$] at the end of chromosomes was shown to extend beyond the DR_L of the HHV-6 genome (Fig. 3). Therefore, the structure of the telomere integrated HHV-6 is as follows: chromosome-subtelomere-$(TTAGGG)_n$-DR_R-U-DR_L-$(TTAGGG)_n$ (Fig. 3a) (Arbuckle et al., 2010).

Delecluse et al. (1993) previously demonstrated the latent telomere-integrated Marek's Disease Virus (MDV) of chickens can also reactivate. MDV integrants were detected as long concatamers suggesting that MDV integration requires initiation of DNA replication and catenation. In contrast, our data show that a single HHV-6 genome integrates immediately following infection. Taken together, these observations suggest the mechanism of integration of the HHV-6/B and MDV are mediated by different mechanisms.

Current diagnostic assays for the detection of reactivated are based on quantitative PCR to determine viral copy number, however quantitative PCR cannot distinguish between actively replicating HHV-6 or latency. Demonstration of catenation/circularization of replicating virus as described in this work can be used in clinical studies to verify that the virus is indeed replicating (Fig. 5).

Telomere position effects (TPE) is characterized by transcriptional repression of telomere adjacent genes through the enrichment of H3K9 methylation and decrease in activating H3K4 methylation emanating from the constitutive heterochromatin state of the telomere (Ottaviani et al., 2008). The epigenetic regulation by TPE is well characterized in *Saccharomyces cerevisiae* (Gottschling et al., 1990; Ottaviani et al., 2008; Tham and Zakian, 2002; Wyrick et al., 1999). The use of reporter systems (GFP, luciferase, URA3) has identified TPE in excess of 20 kbp downstream of the telomere sequence in *S. cerevisiae*. However less established in human cells, Baur et al. (2001) observed a 10 fold decrease in the expression of telomere adjacent luciferase reporter when compared to reporter integrated near the centromere. Moreover, the heterochromatin state of TPE was reversible after treatment of human cells with TSA. This resulted in the suppression of HDACs and transcriptional activation of the luciferase reporter, which parallels the TSA mediated reactivation of HHV-6A from its latent integrated state (Arbuckle et al., 2010). The impact of TPE on HHV-6 and cellular gene expression is unknown. In particular, it is intriguing whether TPE plays a role in transcriptional repression of lytic HHV-6 genes thus maintaining viral latency during integration. Furthermore, it is unknown whether integration of the ~160 kb HHV-6 genome would alter expression of nearby cellular genes due to interruption/alteration of TPE.

Integration of the viral genome may also alter stability of telomeres of the affected chromosome. We thus far have shown that the viral DR_R of the genome is integrated within 5–41 telomere repeats from the end of the chromosome (Figs. 1 and S1) (Arbuckle et al., 2010). The proximity of the ~160 kbp HHV-6 genome integrated between the end of the chromosome and tandem array of telomere repeats suggests that the virus has a minimal impact on the telomere/shelterin complex. However, if the HHV-6 genome were to integrate near the end of the telomere, one would expect progressive shortening of the telomere and the viral genome. Subsequently, this loss may lead to chromosome instability as the result of chromosome fusion, replicative senescence, or the inability of the shelterin complex to bind the non-telomere coding sequence of the virus to form the protective cap at the end of telomere. These intriguing questions are currently being addressed.

The studies presented here and earlier (Arbuckle et al., 2010; Arbuckle and Medveczky, 2011) lead to some important questions across fields of virology, telomere biology, DNA recombination/repair, and inheritance. Future experiments are needed to determine the overall clinical impact of germ-line integrated CIHHV-6.

To conclude, we have provided further results supporting that HHV-6A and HHV-6B are unique among human herpesviruses: they have the potential to specifically integrate into telomeres of chromosomes as described for CIHHV-6 individuals and also

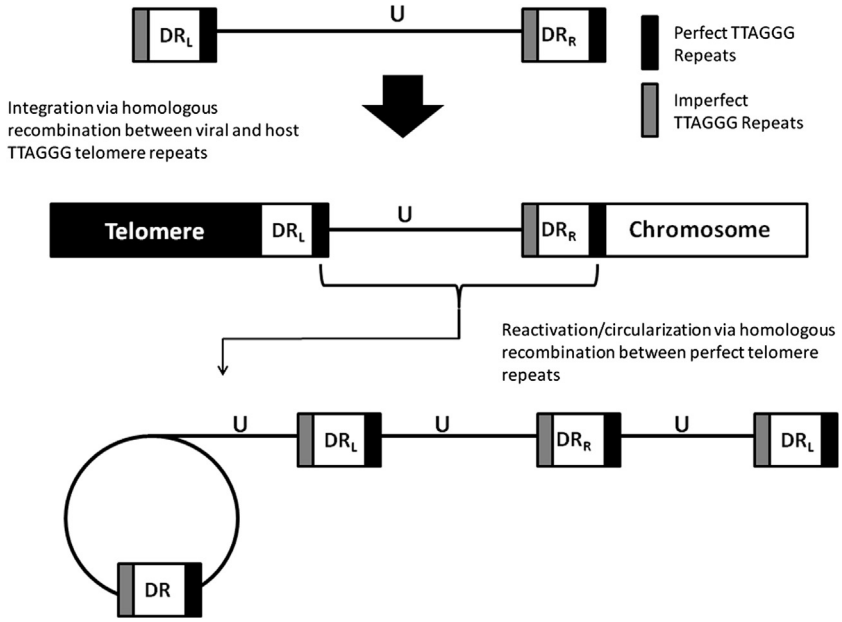

Fig. 5. Proposed model for latent HHV-6 *in vitro* reactivation. During latency, HHV-6A and HHV-6B can integrate into the telomeres during *in vivo* and *in vitro* infection. However, reactivation of integrated HHV-6 can be achieved through culturing of latently integrated cells with TSA, or alternatively, TPA plus hydrocortisone. (b) Reactivation of the integrated HHV-6 results in genome replication through rolling-circle replication.

in vitro under experimental conditions. Moreover, the integrated viral genome is capable of reactivation to produce infectious virions (Arbuckle et al., 2010) and here we designed a PCR-based assay to test clinical specimens for actively replicating HHV-6A and HHV-6B.

Materials and methods

Primary T-cells, cell lines, and viruses

Heparinized peripheral blood from patients with germ-line inherited ClHHV-6 was obtained from the HHV-6 Foundation, after the subjects gave informed consent (Arbuckle et al., 2010). Peripheral blood mononuclear cells (PBMCs) were isolated using Lymphoprep™, according to the manufacturer's protocol. PBMCs were incubated in RPMI-1640 medium containing 10% FBS, 50 μg/ml gentamycin, and 5 μg/ml phytohemagglutinin (PHA, Sigma-Aldrich) for 72-h, followed by culturing in 100 U/μl IL-2 medium. T-cell lines Jjhan (HHV-6 Foundation), and Molt3 (ATCC) were maintained in RPMI-1640 medium containing 10% FBS and 50 μg/ml gentamycin. Human embryonic kidney-293 cells (HEK-293) and HHV-6A *in vitro* integrated cells previously established in our lab (Arbuckle et al., 2010) were maintained in DMEM supplemented with 10% FBS. HHV-6A (U1102 strain) and HHV-6B (Z29 strain) viruses were obtained from Dr. Philip Pellett (Wayne State University).

Infection of cell lines with HHV-6 in vitro to study integration

After removal of dead cells using Lymphoprep™ isotonic density gradient, 10^7 T-cells were infected with HHV-6A (U1102) and HHV-6B (Z29) at 1.0 MOI in 1 ml of RPMI-1640 complete for 2 h at 37°C. Specifically, the T-cell lines Jjhan and Molt3, were infected with HHV-6A and HHV-6B, respectively. Unabsorbed virus was removed by centrifugation for 5 min at 470 × *g*, 25°C (Fisher accuSpin 1R). Cell pellet was resuspended to 10^6 cells/ml and incubated at 37°C, 5% CO_2.

Reactivation of chromosome integrated HHV-6

PBMCs were cultured in RPMI-1640 medium containing 10% FBS and various concentrations of Trichostatin (TSA), or alternatively, 12-O-Tetradecanoyl-13 acetate (TPA) final concentration of 10 ng/ml and 10 μM hydrocortisone as previously described by Arbuckle et al. (2010). DNA was prepared from cells following the time of peak cytopathic effect (5–14 days).

Chromosome-specific PCR for HHV-6B integration

The PCR amplification of HHV-6B integration sites included: 400 ng genomic DNA, 50 μM HHV-6 DR$_R$ chromosome specific primers, 500 μM dNTPs, Expand 20 kb^{PLUS} PCR system (Roche Diagnostics, Indianapolis, IN), 10 X Taq buffer, and final volume was increased to 25 μl with H_2O. Samples were amplified with the Peltier Thermal Cycler PCR (PTC-220, MJ Research Inc, Waltham, Ma) and subjected to the following PCR conditions: 94°C for 2 min, which is then followed by 35 cycles of 94°C for 10 s, 64°C for 30 s, and 68°C for 10 min, and completed with a final extension of 68°C for 7 min. Agarose gel electrophoresis and Southern blot hybridization with telomere, HHV-6, and chromosome specific [γ^{32}P]-ATP-radiolabeled oligonucleotide probes were utilized for identifying DNA bands representing the putative viral-chromosomal DNA junction. Bands were gel extracted with Perfectprep® Gel Cleanup Kit (Eppendorf, Westbury, NY) and cloned with pCR®4-TOPO® (TOPO TA Cloning® Kit for Sequencing, Invitrogen, Carlsbad, *CA*). A minimum of three clones from each sample was sequenced.

Single telomere length analysis (STELA)

Genomic DNA was isolated from PBMCs of patients with inherited HHV-6A and HHV-6B and from HEK-293 cells carrying

integrated HHV-6A (Arbuckle et al., 2010). Oligonucleotide linker (Tellorette-2) containing a single TTAGGG repeat was ligated to the end of the telomere by incubating 60–150 ng of genomic DNA, 60–100 μM of oligonucleotide Telorette-2, and 4.5 U of T4 DNA ligase for 13 h at 35°C. The ligation reaction was then purified through phenol chloroform extraction, ethanol precipitation, and resuspended in 15 μl TE. Serial dilution of Telorette-2-ligated-DNA was amplified with a high fidelity taq polymerase (Expand 20 kb^{PLUS} PCR System, Roche), 25 μM linker annealing primer (Teltail-P1), 25 μM HHV-6 STELA-P2. Cycling conditions were 92°C for 2 min, 27 cycles of 92°C for 15 s, 59°C for 30 s, 68°C 13.5 min or 18 min, and a final extension of 68°C for 7 min. Amplification products were separated through electrophoresis on a 0.8% agarose gel and Southern hybridized with [γ^{32}P]-ATP-radiolabeled telomere oligonucleotide probe and PCR amplified (primers P3+P4) HHV-6 DR$_L$ random primer [α^{32}P]-dATP-radiolabeled probe. Telomere length linked to integrated HHV-6 was then calculated based upon the mean molecular weight of bands co-hybridizing with telomere and HHV-6 DR$_L$ probes.

Reactivation of integrated HHV-6

PBMCs were cultured in RPMI-1640 medium containing 10% FBS and various concentrations of Trichostatin (TSA), or alternatively, 12-O-Tetradecanoyl-13 acetate (TPA) final concentration of 10 ng/ml and 10 μM hydrocortisone as described by Arbuckle et al. (2010).

Primer sequences

Oligonucleotides for chromosome-specific PCR and probe:

HHV-6 DR$_R$: 5′-CATAGATCGGGACTGCTTGAAAGCGC-3′ (Arbuckle et al., 2010)
HHV-6 DR$_R$-probe: 5′-GCGGAGACACATAGCCTTGGCGGGAAGAC-3′
Chromosome 2p: 5′-GAGCTGCGTTTTGCTGAGCAC (Baird et al., 2003)
Chromosome 11q: 5′-CAGACCTTGGAGGCACGGCCTTCG-3′ (Baird et al., 2003)
Chromosome 17p: 5′-AACATCGAATCCACGGATTGCTTTGTGTAC-3′ (Baird et al., 2003)
Chromosome 18q: 5′-CTCATGTCCTCGGTCTCTTGCCTC-3′ (Arbuckle et al., 2010)
Telomere Probe: 5′-TTAGGGTTAGGGTTAGGGTTAGGG-3′ (Arbuckle et al., 2010)

DR$_L$ PCR:

P1: 5′-ATGTGGCGATCATCCAATCAACGG-3′
P2: 5′-AAATGTCTGCGGAAAGGTCAACCG-3′
P3: 5′-CATAGATCGGGACTGCTTGAAAGCGG-3′
P4: 5′- AAATGTCTGCGGAAAGGTCAACCG-3′
HHV-6 DR$_L$ Probe: 5′-CCCCAACGCGCGCGCGCACGC-3′

Oligonucleotides for STELA PCR and probe:

Tellorette-2 (Linker): 5′-TGCTCCGTGCATCTGGCATCTAACCCT-3′ (Baird et al., 2003)
P1-Teltail: 5′-TGCTCCGTGCATCTGGCATC-3′ (Baird et al., 2003)
P2-HHV6 STELA: 5′-AAGGATGGTAGGGTTTAGGGTCGAACC-3′
P3-HHV6 STELA: 5′-CCCTAACACTAATCCTCGCATCCGC-3′
XpYpE2: 5′-TTGTCTCAGGGTCCTAGTG-3′ (Baird et al., 2003)
XpYpB2: 5′-TCTGAAAGTGGACCTATCAG-3′ (Baird et al., 2003)

Acknowledgments We thank Dr. Philip Pellett providing HHV-6A and 6B stocks. This work was supported by a grant from the HHV-6 Foundation and the National Institute of Health 5R01CA111196 for PGM.

Appendix A. Supporting information Supplementary data associated with this article can be found in the online version at http://dx.doi.org/10.1016/j.virol.2013.03.030.

References

Ablashi, D.V., Devin, C.L., Yoshikawa, T., Lautenschlager, I., Luppi, M., Kuhl, U., Komaroff, A.L., 2010. Review Part 3: human herpesvirus-6 in multiple non-neurological diseases. J. Med. Virol. 82, 1903–1910.
Ahlqvist, J., Fotheringham, J., Akhyani, N., Yao, K., Fogdell-Hahn, A., Jacobson, S., 2005. Differential tropism of human herpesvirus 6 (HHV-6) variants and induction of latency by HHV-6A in oligodendrocytes. J. Neurovirol. 11, 384–394.
Arbuckle, J.H., Medveczky, M.M., Luka, J., Hadley, S.H., Luegmayr, A., Ablashi, D., Lund, T.C., Tolar, J., De Meirleir, K., Montoya, J.G., Komaroff, A.L., Ambros, P.F., Medveczky, P.G., 2010. The latent human herpesvirus-6A genome specifically integrates in telomeres of human chromosomes *in vivo* and *in vitro*. PNAS 107, 5563–5568.
Arbuckle, J.H., Medveczky, P.G., 2011. The molecular biology of human herpesvirus-6 latency and telomere integration. Microb. Infect. 13, 731–741.
Asano, Y., Yoshikawa, T., Suga, S., Kobayashi, I., Nakashima, T., Yazaki, T., Kajita, Y., Ozaki, T., 1994. Clinical features of infants with primary human herpesvirus 6 infection (exanthem subitum, roseola infantum). Pediatrics 93, 104–108.
Baird, D.M., Rowson, J., Wynford-Thomas, D., Kipling, D., 2003. Extensive allelic variation and ultrashort telomeres in senescent human cells. Nat. Genet. 33, 203–207.
Baur, J.A., Zou, Y., Shay, J.W., Wright, W.E., 2001. Telomere position effect in human cells. Science (New York, N.Y) 292, 2075–2077.
Borenstein, R., Frenkel, N., 2009. Cloning human herpes virus 6A genome into bacterial artificial chromosomes and study of DNA replication intermediates. PNAS 106, 19138–19143.
Borenstein, R., Zeigerman, H., Frenkel, N., 2010. The DR1 and DR6 first exons of human herpesvirus 6A are not required for virus replication in culture and are deleted in virus stocks that replicate well in T-cell lines. J. Virol. 84, 2648–2656.
Britt-Compton, B., Rowson, J., Locke, M., Mackenzie, I., Kipling, D., Baird, D.M., 2006. Structural stability and chromosome-specific telomere length is governed by cis-acting determinants in humans. Hum. Mol. Genet. 15, 725–733.
Cameron, B., Flamand, L., Juwana, H., Middeldorp, J., Naing, Z., Rawlinson, W., Ablashi, D., Lloyd, A., 2010. Serological and virological investigation of the role of the herpesviruses EBV, CMV and HHV-6 in post-infective fatigue syndrome. J. Med. Virol. 82, 1684–1688.
Caselli, E., Zatelli, M.C., Rizzo, R., Benedetti, S., Martorelli, D., Trasforini, G., Cassai, E., degli Uberti, E.C., Di Luca, D., Dolcetti, R., 2012. Virologic and immunologic evidence supporting an association between HHV-6 and Hashimoto's thyroiditis. PLoS Pathog. 8, e1002951.
Daibata, M., Taguchi, T., Taguchi, H., Miyoshi, I., 1998. Integration of human herpesvirus 6 in a Burkitt's lymphoma cell line. Br. J. Haematol 102, 1307–1313.
De Bolle, L., Naesens, L., De Clercq, E., 2005. Update on human herpesvirus 6 biology, clinical features, and therapy. Clin. Microbiol. Rev. 18, 217–245.
Delecluse, H.J., Schuller, S., Hammerschmidt, W., 1993. Latent Marek's disease virus can be activated from its chromosomally integrated state in herpesvirus-transformed lymphoma cells. EMBO J. 12, 3277–3286.
Dominguez, G., Dambaugh, T.R., Stamey, F.R., Dewhurst, S., Inoue, N., Pellett, P.E., 1999. Human herpesvirus 6B genome sequence: coding content and comparison with human herpesvirus 6A. J. Virol. 73, 8040–8052.
Donati, D., Akhyani, N., Fogdell-Hahn, A., Cermelli, C., Cassiani-Ingoni, R., Vortmeyer, A., Heiss, J.D., Cogen, P., Gaillard, W.D., Sato, S., Theodore, W.H., Jacobson, S., 2003. Detection of human herpesvirus-6 in mesial temporal lobe epilepsy surgical brain resections. Neurology 61, 1405–1411.
Gompels, U.A., Nicholas, J., Lawrence, G., Jones, M., Thomson, B.J., Martin, M.E., Efstathiou, S., Craxton, M., Macaulay, H.A., 1995. The DNA sequence of human herpesvirus-6: structure, coding content, and genome evolution. Virology 209, 29–51.
Gottschling, D.E., Aparicio, O.M., Billington, B.L., Zakian, V.A., 1990. Position effect at S. cerevisiae telomeres: reversible repression of Pol II transcription. Cell 63, 751–762.
Hall, C.B., Caserta, M.T., Schnabel, K., Shelley, L.M., Marino, A.S., Carnahan, J.A., Yoo, C., Lofthus, G.K., McDermott, M.P., 2008. Chromosomal integration of human herpesvirus 6 is the major mode of congenital human herpesvirus 6 infection. Pediatrics 122, 513–520.
Jacob, R.J., Morse, L.S., Roizman, B., 1979. Anatomy of herpes simplex virus DNA. XII. Accumulation of head-to-tail concatemers in nuclei of infected cells and their role in the generation of the four isomeric arrangements of viral DNA. J. Virol. 29, 448–457.
Jarrett, R.F., Gledhill, S., Qureshi, F., Crae, S.H., Madhok, R., Brown, I., Evans, I., Krajewski, A., O'Brien, C.J., Cartwright, R.A., et al., 1988. Identification of human herpesvirus 6-specific DNA sequences in two patients with non-Hodgkin's lymphoma. Leukemia 2, 496–502.

Jones, C.M., Dunn, H.G., Thomas, E.E., Cone, R.W., Weber, J.M., 1994. Acute encephalopathy and status epilepticus associated with human herpes virus 6 infection. Dev. Med. Child Neurol. 36, 646–650.
Lauzon, W., Sanchez Dardon, J., Cameron, D.W., Badley, A.D., 2000. J. Flow cytometric measurement of telomere length. Cytometry 15, 159–164.
Leong, H.N., Tuke, P.W., Tedder, R.S., Khanom, A.B., Eglin, R.P., Atkinson, C.E., Ward, K.N., Griffiths, P.D., Clark, D.A., 2007. The prevalence of chromosomally integrated human herpesvirus 6 genomes in the blood of UK blood donors. J. Med. Virol. 79, 45–51.
Luppi, M., Marasca, R., Barozzi, P., Ferrari, S., Ceccherini-Nelli, L., Batoni, G., Merelli, E., Torelli, G., 1993. Three cases of human herpesvirus-6 latent infection: integration of viral genome in peripheral blood mononuclear cell DNA. J. Med. Virol. 40, 44–52.
Lusso, P., Crowley, R.W., Malnati, M.S., Di Serio, C., Ponzoni, M., Biancotto, A., Markham, P.D., Gallo, R.C., 2007. Human herpesvirus 6A accelerates AIDS progression in macaques. PNAS 104, 5067–5072.
Lusso, P., Ensoli, B., Markham, P.D., Ablashi, D.V., Salahuddin, S.Z., Tschachler, E., Wong-Staal, F., Gallo, R.C., 1989. Productive dual infection of human CD4+ T lymphocytes by HIV-1 and HHV-6. Nature 337, 370–373.
Martin, M.E., Thomson, B.J., Honess, R.W., Craxton, M.A., Gompels, U.A., Liu, M.Y., Littler, E., Arrand, J.R., Teo, I., Jones, M.D., 1991. The genome of human herpesvirus 6: maps of unit-length and concatemeric genomes for nine restriction endonucleases. J. Gen. Virol. 72 (Pt 1), 157–168.
Nacheva, E.P., Ward, K.N., Brazma, D., Virgili, A., Howard, J., Leong, H.N., Clark, D.A., 2008. Human herpesvirus 6 integrates within telomeric regions as evidenced by five different chromosomal sites. J. Med. Virol. 80, 1952–1958.
Okuno, T., Takahashi, K., Balachandra, K., Shiraki, K., Yamanishi, K., Takahashi, M., Baba, K., 1989. Seroepidemiology of human herpesvirus 6 infection in normal children and adults. J. Clin. Microbiol. 27, 651–653.
Ottaviani, A., Gilson, E., Magdinier, F., 2008. Telomeric position effect: from the yeast paradigm to human pathologies? Biochimie 90, 93–107.
Pellett, P.E., Roizman, B., 2007. The family herpesviridae: a brief introduction In: Knipe, David M., Howley, Peter M., Griffin, Diane E., Lamb, Robert A., Straus, Stephen E., Martin, Malcolm A., Roizman, Bernard (Eds.), Field's Virology. Lippincott Williams, Philadelphia, PA, pp. 2481.
Poffenberger, K.L., Roizman, B., 1985. A noninverting genome of a viable herpes simplex virus 1: presence of head-to-tail linkages in packaged genomes and requirements for circularization after infection. J. V Virol. 53, 587–595.
Salahuddin, S.Z., Ablashi, D.V., Markham, P.D., Josephs, S.F., Sturzenegger, S., Kaplan, M., Halligan, G., Biberfeld, P., Wong-Staal, F., Kramarsky, B., et al., 1986. Isolation of a new virus, HBLV, in patients with lymphoproliferative disorders. Science (New York, N.Y.) 234, 596–601.
Severini, A., Sevenhuysen, C., Garbutt, M., Tipples, G.A., 2003. Structure of replicating intermediates of human herpesvirus type 6. Virology 314, 443–450.
Strenger, V., Aberle, S.W., Wendelin, G., Pfurtscheller, K., Nacheva, E.P., Zobel, G., Nagel, B., 2010. Chromosomal integration of the HHV-6 genome as a possible cause of HHV-6 detection in cardiac tissues. J. Clin. Pathol. 63, 1129–1130.
Tham, W.H., Zakian, V.A., 2002. Transcriptional silencing at Saccharomyces telomeres: implications for other organisms. Oncogene 21, 512–521.
Ward, K.N., Leong, H.N., Nacheva, E.P., Howard, J., Atkinson, C.E., Davies, N.W., Griffiths, P.D., Clark, D.A., 2006. Human herpesvirus 6 chromosomal integration in immunocompetent patients results in high levels of viral DNA in blood, sera, and hair follicles. J. Clin. Microbiol. 44, 1571–1574.
Ward, K.N., Thiruchelvam, A.D., Couto-Parada, X., 2005. Unexpected occasional persistence of high levels of HHV-6 DNA in sera: detection of variants A and B. J. Med. Virol. 76, 563–570.
Wyrick, J.J., Holstege, F.C., Jennings, E.G., Causton, H.C., Shore, D., Grunstein, M., Lander, E.S., Young, R.A., 1999. Chromosomal landscape of nucleosome-dependent gene expression and silencing in yeast. Nature 402, 418–421.
Yamanishi, K., Okuno, T., Shiraki, K., Takahashi, M., Kondo, T., Asano, Y., Kurata, T., 1988. Identification of human herpesvirus-6 as a causal agent for exanthem subitum. Lancet 1, 1065–1067.
Yamashita, N., Morishima, T., 2005. HHV-6 and seizures. Herpes 12, 46–49.
Yao, K., Crawford, J.R., Komaroff, A.L., Ablashi, D.V., Jacobson, S., 2010. Review part 2: human herpesvirus-6 in central nervous system diseases. J. Med. Virol. 82, 1669–1678.
Zerr, D.M., Meier, A.S., Selke, S.S., Frenkel, L.M., Huang, M.L., Wald, A., Rhoads, M.P., Nguy, L., Bornemann, R., Morrow, R.A., Corey, L., 2005. A population-based study of primary human herpesvirus 6 infection. N. Engl. J. Med. 352, 768–776.